

Absolute measurement of β_{eff} based on Feynman- α experiments and the two-region model in the IPEN/MB-01 research reactor

Renato Y.R. Kuramoto, Adimir dos Santos *, Rogério Jerez, Ricardo Diniz

Instituto de Pesquisas Energéticas e Nucleares, IPEN/CNEN-SP, Av. Prof. Lineu Prestes, 2242 Cidade Universitária, 05508-000 Pinheiros, São Paulo, SP, Brazil

Received 8 January 2007; received in revised form 15 February 2007; accepted 15 February 2007
Available online 16 April 2007

Abstract

A new methodology for absolute measurement of the effective delayed neutron fraction β_{eff} based on Feynman- α experiments and the two-region model was developed. This method made use of Feynman- α experiments and the two-region model. To examine the present methodology, a series of Feynman- α experiments were conducted at the IPEN/MB-01 research reactor facility. In contrast with other techniques like the slope method, Nelson-number method and ^{252}Cf -source method, the main advantage of this new methodology is to obtain β_{eff} with the required accuracy and without knowledge of any other parameter. By adopting the present approach, β_{eff} was measured with a 0.67% uncertainty. In addition, the prompt neutron generation time, Λ , and other parameters, was also obtained in an absolute experimental way. In general, the measured parameters are in good agreement with the values found from frequency analysis experiments. The theory–experiment comparison for the β_{eff} measured in this work shows that JENDL3.3 presented the best agreement (within 1%). The reduction of the ^{235}U thermal yield as proposed by Okajima and Sakurai is completely justified according to the β_{eff} measurements performed in this work.

© 2007 Elsevier Ltd. All rights reserved.

1. Introduction

Since 1990, it has been observed that delayed neutron data uncertainties may result in undesirable conservatism in the design and operation of nuclear reactor control systems (D'Angelo, 2002). Among these data, the effective delayed neutron fraction β_{eff} is an important safety parameter of nuclear reactors because it is equal to the increment between delayed and prompt critical.

The main objective has been to determine whether or not the currently database is sufficiently accurate to predict the measured effective delayed neutron fraction, β_{eff} , for a wide variety of critical assemblies. A target accuracy of $\pm 3\%$ was requested for β_{eff} calculations (Rudstan et al., 2002; D'Angelo and Rowlands, 2002), in way that β_{eff} values must be measured with an experimental error of less

than 3% (Sakurai et al., 1999). In order to improve the prediction accuracy of the β_{eff} , programs of international benchmarks experiments have been planned in different. However, the experimental data of β_{eff} for thermal systems (Van der Marck et al., 2004; Van der Marck, 2006), today available, cannot offer sufficient quality and quantity to predict the β_{eff} with the required accuracy. A literature survey shows that the available experiments related to β_{eff} and/or $\beta_{\text{eff}}/\Lambda$ were performed in the following facilities: Stacy (Tonoike et al., 2002), Winco (Spriggs, 1977), Sheba-II (Butterfield, 1994), Proteus (Williams et al., 1996), TCA (Nakajima, 2001), SHE-8 (Takano et al., 1985; Kaneko et al., 1988), MISTRAL-1 (Litaize and Santamarina, 2001) and IPEN/MB-01 (dos Santos et al., 2006). For the Stacy, Winco, Sheba-II and Proteus, the reported measured quantity is α , which is linked to β_{eff} at delayed critical through $\alpha_0 = \alpha(\rho = 0) = \beta_{\text{eff}}/\Lambda$. The uncertainties in the α value measurements are 1.6% for Stacy, 0.03% for Winco, 1.8% for Sheba-II, and 0.6% for Proteus. Only the TCA, SHE-8, MISTRAL-1 and IPEN/MB-01 experiments,

* Corresponding author. Tel.: +55 11 3816 9396x246; fax: +55 11 3816 9423.

E-mail address: asantos@ipen.br (A. dos Santos).

report measured values of β_{eff} , and their respective uncertainties are 2.2%, 4.6%, 1.6% and 0.9%. The number of experiments related to β_{eff} is quite small. In such a way, a collaborative effort to improve the β_{eff} measurements in thermal systems has been recommended.

Nowadays, different β_{eff} measurement techniques have been applied (Rudstan et al., 2002; Fort et al., 2002). However, all these techniques cannot directly give the β_{eff} , but they yield it using several parameters. The most common parameters are: adjoint fluxes, spatial-correction factors, fission rates, reactivity, neutron source strength and detector efficiency. Among these parameters, the fission rate is measured, while semi-experimental values are obtained for most of the other parameters by combination of measured results and calculated corrections. Uncertainties of these parameters are critical uncertainty sources in these techniques. Typical uncertainties on the measured and semi-experimental parameters of β_{eff} range from 1.20% to 3.09% (Fort et al., 2002). In addition, the Diven factor is common to all techniques excepting the Cf-source method and it introduces an uncertainty in measured β_{eff} values of about 1.3% (D'Angelo and Rowlands, 2002). It is apparent that when a physical quantity needs to be known to a few-percent accuracy then an absolute experimental determination is essential.

For these reasons, a new methodology for absolute measurement of the effective delayed neutron fraction β_{eff} is proposed. This method made use of Feynman- α experiments (Feynman et al., 1956; Uhrig, 1970) and the two-region model (Spriggs et al., 1997). By adopting this approach, values for β_{eff} , and other kinetic parameters may be obtained without any calculations or other experiments results. Consequently, the accuracy in β_{eff} is improved and the proposed target accuracy may be reached. In summary, several Feynman- α distributions were recorded in the IPEN/MB-01 Research Reactor facility (dos Santos et al., 1999, 2004), in a very large range of subcritical reactivity (nearly from -500 pcm to $-25,000$ pcm). As predicted by the two-region model, at subcritical levels above -3000 pcm two exponential components could be observed in Feynman- α distributions recorded in reflector region. However, the value of this second exponential term cannot be extracted because of detector dead time effects. By fitting the α versus inverse count rate curve through the two-region model, β_{eff} and other kinetic parameters were estimated. Using this methodology, the β_{eff} could be evaluated with the required accuracy and without knowledge of any other parameter.

2. The two-region model

One of the most important classes of nuclear reactors are reflected reactors. However, several experimental data clearly show that the kinetic behavior of some types of reflected systems cannot be adequately explained using the standard one-region point kinetic model (Bell and Glasstone, 1970). In particular, the departure of zero-

power transfer function of some types of reflected systems from the standard model at high frequencies (Diniz, 2005), the multiple decay modes observed in Rossi- α and pulsed neutron experiments (Karam, 1964, 1965; Busch and Spriggs, 1994; Brunson and Huber, 1975; Brunson, 1975), and the nonlinear behavior of prompt neutron decay constant versus reactivity curve (Brunson, 1975; Gamble, 1960; Long, 1965; Coats, 1967; Price, 1970). All these measurements revealed a significant deviation from the one-region point kinetics approximation applied in conventional systems. It was concluded that in some reflected systems, the one-region point kinetic behavior is expected to be no longer valid. However, all these anomalies can be explained through the two-region model.

The two-region model was developed on previous works by Avery (1958), Avery et al. (1958), Cohn (1961) and Cohn (1962) and further simplified by Spriggs et al. (1997). This model describes the time-dependent behavior of multiplying systems comprised of two distinct regions, the core and a non-multiplying, source-free reflector. Each region is characterized by a multiplication factor, and a neutron lifetime. Neutrons in the core region can undergo absorption or fission reactions and are allowed to leak to the reflector. Neutrons in the reflector are either absorbed or leak back to the core or are lost from the system. From these considerations, a reflected system can be described by the following set of coupled differential equations (Cohn, 1962; Spriggs et al., 1997):

$$\frac{dN_c}{dt} = [k_c(1 - \beta_{\text{eff}}) - 1] \left(\frac{N_c}{\tau_c} \right) + f_{rc} \left(\frac{N_r}{\tau_r} \right) + \sum \lambda_i c_i + S, \quad (1)$$

$$\frac{dN_r}{dt} = f_{cr} \left(\frac{N_c}{\tau_c} \right) - \left(\frac{N_r}{\tau_r} \right), \quad (2)$$

$$\frac{dc_i}{dt} = k_c \beta_i \left(\frac{N_c}{\tau_c} \right) - \lambda_i c_i, \quad (3)$$

where the definitions of the quantities are taken from Spriggs et al. (1997): N_c the adjoint-weighted total number of neutrons in the core region; N_r the adjoint-weighted total number of neutrons in the reflector region; k_c the multiplication factor of the core region; β_{eff} the effective delayed neutron fraction; τ_c the adjoint-weighted neutron lifetime in the core region; τ_r the adjoint-weighted neutron lifetime in the reflector region; f_{cr} the fraction of neutrons that leak from the core into the reflector; f_{rc} the fraction of neutrons that leak from the reflector back into the core; $f = f_{cr} \cdot f_{rc}$ the fraction of core neutrons returned to the core after having leaked into the reflector; c_i the adjoint-weighted concentration of the i th precursor group; β_i the delayed neutron fraction of the i th precursor group; λ_i the decay constant of the i th precursor group; and S the adjoint-weighted intrinsic/external neutron source rate in the core.

The Laplace-transform method (Bell and Glasstone, 1970) provides a standard way of deriving the inhour equation. By applying this approach to Eqs. (1)–(3), the poles ω of the Laplace transform of $N_c(s)$, are the solution of the reflected-core inhour equation, which can be written as

$$\rho = \frac{k_c + f - 1}{k_c} = \omega A_c + \sum \frac{\beta_i \omega}{\omega + \lambda_i} + \frac{\omega f A_r}{\tau_r \omega + 1}, \quad (4)$$

where A_c is the core’s prompt-neutron generation time and A_r is the reflector’s prompt-neutron generation. These quantities can be related to the neutrons lifetimes in core and reflector region through the following expressions:

$$A_c = \frac{\tau_c}{k_c}, \quad (5)$$

$$A_r = \frac{\tau_r}{k_c}. \quad (6)$$

The same expression for the reflected-core inhour equation, can be derived taking the poles ω of the Laplace transform of Eq. (2). Eq. (4) can be written in a more convenient way as

$$\begin{aligned} \rho &= \omega_k A_c + \sum_i \frac{\beta_i \omega_k}{\omega_k + \lambda_i} + \frac{\beta_r \omega_k}{\omega_k + \lambda_r} \\ &= \omega_k A_c + \sum_{i,r} \frac{\beta_i \omega_k}{\omega_k + \lambda_i}, \end{aligned} \quad (7)$$

where, β_r and λ_r are defined, in a purely mathematical way, as

$$\beta_r = f \frac{A_r}{\tau_r}, \quad (8)$$

and

$$\lambda_r = \frac{1}{\tau_r}. \quad (9)$$

According to Eq. (7), it is observed that when f approaches zero the reflected-core inhour equation collapses to the inhour equation for a bare reactor (Bell and Glasstone, 1970). On the other hand, when f is greater than zero, an extra term associated with the reflector appears in the equation.

For the case of six precursor groups (i.e., $i = 6$), the reflected-core inhour equation is a polynomial equation of eighth order. Thus, for every value of ρ there are eight roots ω_j . In contrast to the one-region inhour equation, Eq. (7) presents an additional root, ω_8 , which varies from $-1/\tau_r$ to $-\infty$. Fig. 1 is a qualitative plot of the reflected-core inhour equation.

The seventh root of the reflected-core inhour equation varies from $-\lambda_6$ to $-1/\tau_r$. At reactivities in the vicinity of delayed critical follow the asymptote:

$$\omega_7 = \frac{\rho - \beta_{eff}}{\Lambda}, \quad (10)$$

and at critical state $\omega_7 = \beta_{eff}/\Lambda$. On the other hand, at large subcritical levels, ω_7 goes asymptotically to $-1/\tau_r$. Thus, it is evident that at some subcritical reactivity the linear behavior of ω_7 given by Eq. (10) is lost. From this point the one-region model is not valid and the two-region model must be applied. This departure from Eq. (10) at large subcritical levels is a quantitative way to validate the two-region model.

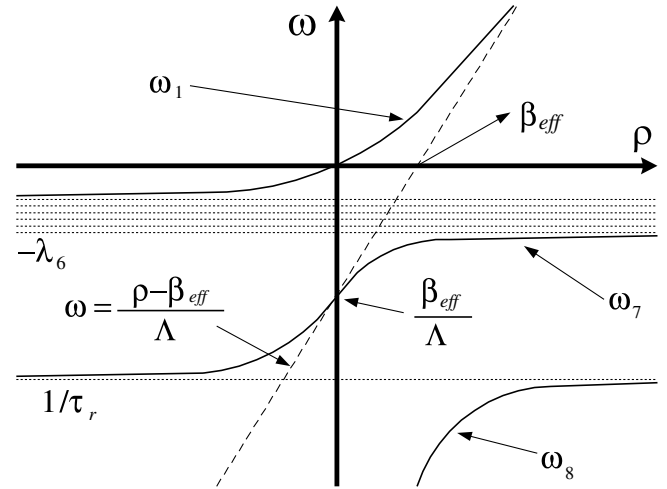


Fig. 1. Qualitative plot of the roots of the reflected-core inhour equation. The plot is not drawn to scale.

3. The reflected-core Feynman- α distribution

The Feynman- α technique is based on the measurement of the ratio of the variance to the mean of the number of counts collected in a fixed time interval T . If it was repeatedly measure the number of counts c occurring in a given time interval, the variance-to-mean ratio of the number of counts is given by Uhrig (1970):

$$\frac{\text{variance}}{\text{mean}} = \frac{\bar{c}^2 - \bar{c}^2}{\bar{c}}, \quad (11)$$

where \bar{c} represents the average number of counts in the time interval T .

The Feynman- α distribution can be derived from the Rossi- α distribution through the following integral (Uhrig, 1970):

$$\frac{c(c-1)}{2} = \varepsilon F \int_{t_2=0}^T \int_{t_1=0}^{t_2} p_{\text{Rossi}}(t_1, t_2) dt_1 dt_2, \quad (12)$$

where F is the average fission rate and ε is the detector efficiency. The left-hand side represents the number of pairs of counts expected in the interval T , and $p_{\text{Rossi}}(t_1, t_2)$ is the total probability of a pair of counts in dt_1 and dt_2 given by the Rossi- α distribution. The reflected core Rossi- α distributions recorded in the core and reflector region can be, respectively, written as

$$\begin{aligned} p_{\text{Rossi}}^c(\tau) &= A^c \sum_{k=7,8} \frac{\frac{\rho}{\omega_k}}{A_c + \frac{\beta_r \lambda_r}{(\omega_k + \lambda_r)^2}} e^{\omega_k \tau} + \text{BG} \\ &= A^c (N_7^c e^{\omega_7 \tau} + N_8^c e^{\omega_8 \tau}) + \text{BG}, \end{aligned} \quad (13)$$

and

$$\begin{aligned} p_{\text{Rossi}}^r(\tau) &= A^r \sum_{k=7,8} \frac{\lambda_r}{\omega_k + \lambda_r} \frac{\frac{\rho}{\omega_k}}{A_c + \frac{\beta_r \lambda_r}{(\omega_k + \lambda_r)^2}} e^{\omega_k \tau} + \text{BG} \\ &= A^r (N_7^r e^{\omega_7 \tau} + N_8^r e^{\omega_8 \tau}) + \text{BG}, \end{aligned} \quad (14)$$

where $\tau = t_2 - t_1$ is the elapsed time between two neutron counts. The quantity A^c and A^r are proportionality constants, with dimensions of inverse of time, which relates adjoint-weighted total number of neutrons to the experimental Rossi- α distributions recorded in the core and reflector regions, respectively. The BG term can be written as the product of the average fission rate and the detector efficiency, and experimentally represents the uncorrelated or random component which is added to the Rossi- α distribution as a background component.

By substituting $p_{\text{rossi}}(t_1, t_2)$ in the form of $N_7^{c,r} e^{\omega_7(t_2-t_1)} + N_8^{c,r} e^{\omega_8(t_2-t_1)} + \text{BG}$, into Eq. (12) and solving the integrals, we obtain:

$$\frac{c(\bar{c}-1)}{2} = -A^{c,r} F \varepsilon T \left[\frac{N_7^{c,r}}{\omega_7} \left(1 + \frac{1 - e^{\omega_7 T}}{\omega_7 T} \right) + \frac{N_8^{c,r}}{\omega_8} \left(1 + \frac{1 - e^{\omega_8 T}}{\omega_8 T} \right) \right] + \frac{(F \varepsilon T)^2}{2}. \quad (15)$$

Since the product $F \varepsilon T$ is equal to the average number of counts \bar{c} in the interval T , we can rearrange Eq. (15) to obtain:

$$Y = \frac{\bar{c}^2 - \bar{c}}{\bar{c}} - 1 = -2A^{c,r} \left[\frac{N_7^{c,r}}{\omega_7} \left(1 + \frac{1 - e^{\omega_7 T}}{\omega_7 T} \right) + \frac{N_8^{c,r}}{\omega_8} \left(1 + \frac{1 - e^{\omega_8 T}}{\omega_8 T} \right) \right], \quad (16)$$

where Y is the reflected core Feynman- α distribution. Therefore, explicit expressions for the Feynman- α distribution recorded in the core and reflector region can be obtained by substituting the core amplitudes N_7^c and N_8^c , and the reflector amplitudes N_7^r and N_8^r , given by Eqs. (13) and (14), into Eq. (16), respectively.

The standard deviation σ_Y of the Y -value can be approximately derived from those of the sample variance and mean of the normal distribution (Jammes et al., 2002):

$$\omega_{7,8} = \frac{1}{2A_c A_r (1-f)} \left\{ \frac{-[(1-\rho)(A_c + fA_r) + A_r(1-f)(\beta_{\text{eff}} - \rho)] \pm \sqrt{\{(1-\rho)(A_c + fA_r) + A_r(1-f)(\beta_{\text{eff}} - \rho)\}^2 - 4A_c A_r (1-f)(1-\rho)(\beta_{\text{eff}} - \rho)}}{2} \right\}, \quad (20)$$

$$\sigma_Y = \frac{1+Y}{\sqrt{N}} \sqrt{\frac{1+Y}{\bar{c}} + 2}, \quad (17)$$

where N is the number of samples (i.e. the number of counts) for a given time gate T .

In contrast to one-region model, the reflected core Feynman- α distribution shows two exponential terms. The first exponential term, which is governed by the ω_7 -eigenvalue, is the well-known Feynman- α distribution derived from the one-region model, and the ω_7 root is the familiar prompt

neutron decay constant, α . This term physically represents the prompt neutrons that multiply within the core region on a time scale corresponding to the prompt-neutron generation time in the bare reactor core, A_c . The second exponential term, driven by ω_8 , is an additional term associated with that fraction of prompt neutrons that leak from the core into the reflector and then re-enter the core region where they further propagate the prompt-neutron chains by inducing additional fissions. This process occurs on the time scale of the prompt-neutron generation time of the integral system A . The prompt neutron generation time A can be written as a sum of two components via the following relation (Spriggs et al., 1997):

$$A = A_c + fA_r, \quad (18)$$

This equation is valid for reflected systems where the neutron lifetime in reflector region is sufficiently small, which corresponds to $\tau_r \omega_j \ll 1$.

Has been observed that counting loss originates from dead time due to pulse-type neutron detector and counting circuits lead to considerable distortions in the uncorrelated part of Feynman- α distribution. In fact, the Y -value can be sometimes negative because the dead time effect at high counting rates. In order to overcome the undesirable dead time effect, assuming a non-paralyzable counting system, Yamane proposed the following improved formula (Yamane, 1996):

$$Y_d = Y - 2Rd, \quad (19)$$

where the uncorrelated part depends linearly on the dead time d and the counting rate R .

In practice, the delayed neutrons can be neglected because they are virtually constant over the time intervals used in the Feynman- α experiments (Feynman et al., 1956; Uhrig, 1970). By adopting this assumption, the ω_7 and ω_8 roots can be obtained from the reflected core inhour equation (Eq. (4)) by assuming $\omega \gg \lambda_i$. Thus, the following equation is derived:

where the positive and negative signs go with ω_7 and ω_8 , respectively. This equation shows clearly that the relationship between the roots ω_7 and ω_8 , and reactivity is not linear.

Since we are only interested in relative changes in reactivity level due to changes in the control rod position, the reactivity ρ in Eq. (20) can be obtained through the neutron source multiplication method (NSMM) (Misawa and Unesaki, 2003; Shi et al., 2005). NSMM is a well-known experimental method, in which the subcritical reactivity ρ is related to the neutron count rate C as follow:

$$\rho = \frac{1}{1 - \frac{c}{\varepsilon S}}, \quad (21)$$

where ε is the detector efficiency and S the source intensity. Even if the product εS is unknown, by monitoring the neutron count rate of a detector, one can evaluate the deviation of the actual reactivity from the reference reactivity.

Through Eqs. (13), (14) and (20), it is possible to study quantitatively the experimental behavior of the roots ω_7 and ω_8 , and the amplitudes $N_7^{r,c}/\omega_7$ and $N_8^{r,c}/\omega_8$ with the subcritical reactivity. Firstly, as indicated in Fig. 1, as reactivity becomes more negative, the magnitude of ω_8 root increases drastically, while the ω_7 root goes asymptotically to $-1/\tau_r$. Evaluating the core correlated amplitudes, it was noticed that the N_7^c/ω_7 is dominant at subcritical levels near the delayed critical condition. In fact, only at large subcritical levels N_7^c/ω_7 can be slightly smaller than N_8^c/ω_8 . However, this small difference is not enough to allow an experimental observation. Therefore, the correlated term driven by ω_8 cannot be easily identified in Feynman- α distributions recorded in core region. In reflector region, the behavior of the amplitudes is completely opposite to that observed in core region. Firstly, according to Eq. (14), the ω_8 root is always greater in magnitude than $\lambda_r = 1/\tau_r$ and due to the term $\lambda_r/(\omega_8 + \lambda_r)$, N_8^r/ω_8 becomes negative. Near the critical condition, Eqs. (13) and (14) indicates that there is a competition between the two correlated components in the Feynman- α distributions recorded in reflector region. On the other hand, the magnitude of N_8^r/ω_8 decreases with the reactivity and approaches asymptotically zero for deep subcritical levels. In such a way, it would be expected that two correlated components could be observed in reflector measurements near the critical state. However, experimentally, due to the relatively high count rates near the delayed critical condition, the dead time losses distort considerably the first channels of the Feynman- α distributions leading to negative Y -values. Thus, the negative exponential component cannot be easily separated from the dead time effect. In summary, the $N_7^{r,c}/\omega_7$ is often dominant over $N_8^{r,c}/\omega_8$, and it is expected that only one correlated component could be observed in Feynman- α distributions recorded in core and reflector regions.

4. The IPEN/MB-01 research reactor and core configurations

To examine the present methodology, a series of Feynman- α experiments were conducted at the IPEN/MB-01 research reactor facility, located in the city of São Paulo, Brazil. The IPEN/MB-01 reactor is a zero-power critical facility especially designed for measurements of a wide variety of reactor physics parameters to be used as benchmark experimental data. The reactor reached its first criticality on November 9, 1988, and since then it has been utilized for basic reactor physics research and as an instructional laboratory system. The reactor core consists of a

28×26 array out of which 680 are fuel rods inside a water tank. The remaining 48 positions are holes, which are used to fix the guide tubes for the control and safety rods. The pitch of the rods is 15.0 mm, which is close to the optimal pitch (maximum k_∞). This feature favors the neutron thermal energy region and mainly the ^{235}U events. Fuel rods are constituted of a stainless steel (type 304) cladding containing UO_2 enriched to 4.3%. Each one of the control and safety banks is composed of 12 rods held together and supported by a control mechanism above the moderator tank. The absorber rods are clad by SS-304. The control rods are filled with an alloy of Ag–In–Cd, while the safety rods are filled with B_4C powder. The maximum operating power of the facility is limited to 100 W. A complete description of the IPEN/MB-01 reactor can be found in dos Santos et al. (1999, 2004).

Feynman- α distributions were recorded in two different core configurations. Fig. 2 displays a schematic view of each configuration and the respective detector locations. The first configuration, illustrated in Fig. 2a, was loaded in order to perform Feynman- α measurements near the delayed critical condition and obtain $\beta_{\text{eff}}/\Lambda$. For this purpose, one small BF_3 neutron detector of 10 mm diameter \times 150 mm height and sensitivity of 2.1 cps/nv was placed in the center of the active core. It is known that in a subcritical core, the power level is determined by the strength of the external neutron source. Thus, in this first configuration, the reactor was driven by its own intrinsic source in order to avoid high count rates, and consequently high dead time losses in the BF_3 detector.

The second core configuration is showed in Fig. 2b. In such configuration, eight burnable poison rods were loaded in the core in order to remove the reactivity excess. Each poison rod is geometrically identical to the fuel rods, but is filled with 52 pellets of $\text{Al}_2\text{O}_3\text{-B}_4\text{C}$ with 40.53 mg of Boron per cubic centimeter. Through this core configuration, when the control and safety rods were fully inserted, the subcritical reactivity was approximately $-25,000$ pcm. In such a way, Feynman- α distributions can be recorded in a very large range of subcritical reactivity, nearly from -500 pcm to $-25,000$ pcm. On the other hand, this large subcritical interval leads to a significant variation in the neutron flux, and consequently in the detector count rate. In order to allow an accurate measurement of the Feynman- α distributions in a reasonable length of time, two detectors with different sensitivities were positioned in the reflector region as illustrated in Fig. 2b. In addition, to increase the count rate of the detectors to a more reasonable value, the startup source (Am–Be, 1Ci) was inserted in the bottom of the core to drive the system. The startup source position can be observed in Fig. 3, which shows the side view of the reactor core. At large subcritical levels, a ^3He detector, whose size and sensitivity were 42 cm in length and 2.6 cm in diameter and 54.3 cps/nv, was employed. For measurements at near critical conditions, where neutron flux is higher, less sensitive (12.9 cps/nv) boron-lined detector of 10 cm diameter \times 33 cm height

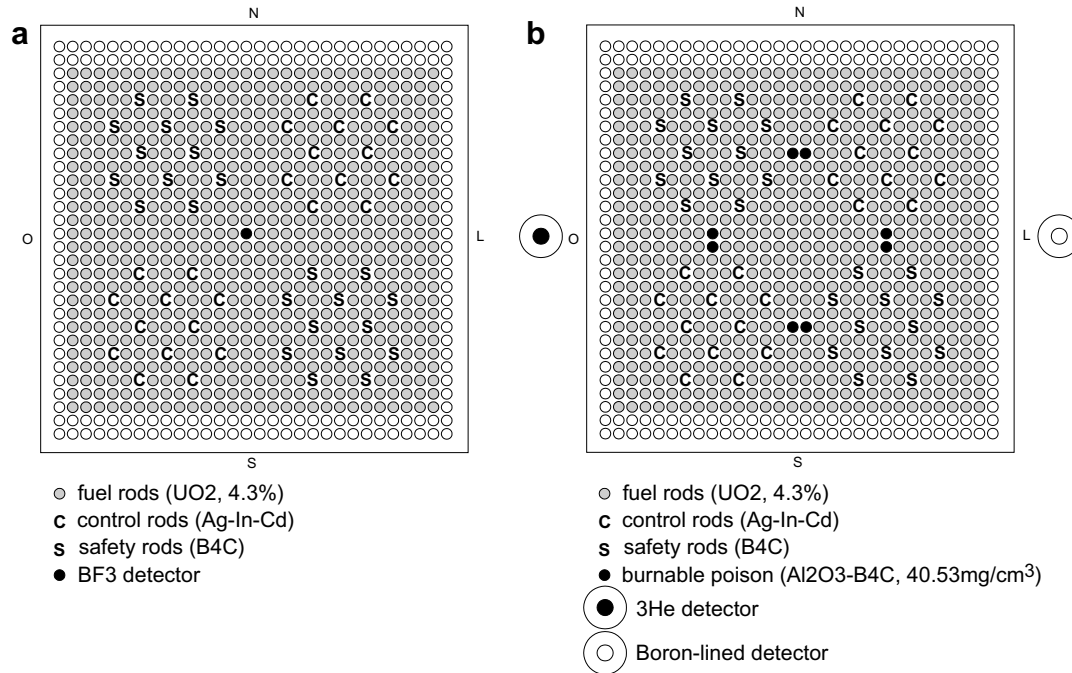


Fig. 2. IPEN/MB-01 core configurations. (a) BF₃ detector positioned in the center of the active core. (b) Eight burnable poison rods positioned in the active core and three different detectors in the reflector region.

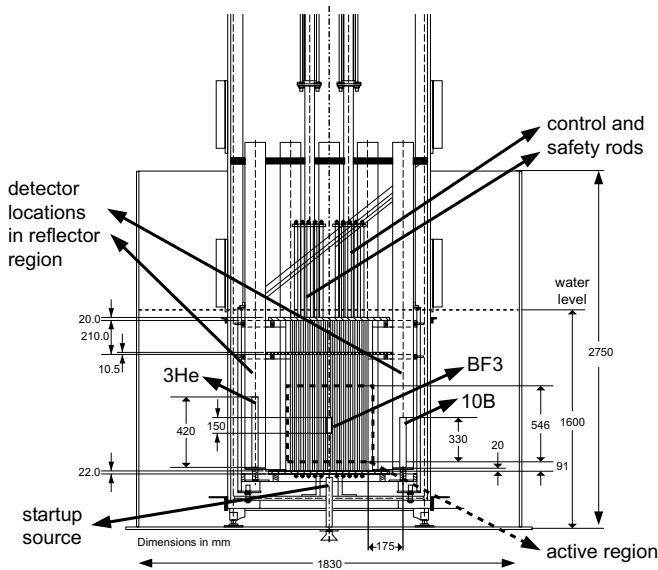


Fig. 3. Side view of the IPEN/MB-01 reactor core. The three neutron detectors are not on scale.

was used to avoid high count rates and large dead time effects.

In general, the system used to record the Feynman- α distributions comprises of a pulse type neutron detector, a pre-amplifier, an amplifier, a discriminator and a multi-channel analyzer. A block diagram of the electronic chain is illustrated in Fig. 4. The combined high voltage supply and amplifying electronics discriminate the neutron pulses from the gamma pulses and amplifies and shapes each neutron pulse into a NIM fast negative logic pulse of 25 ns

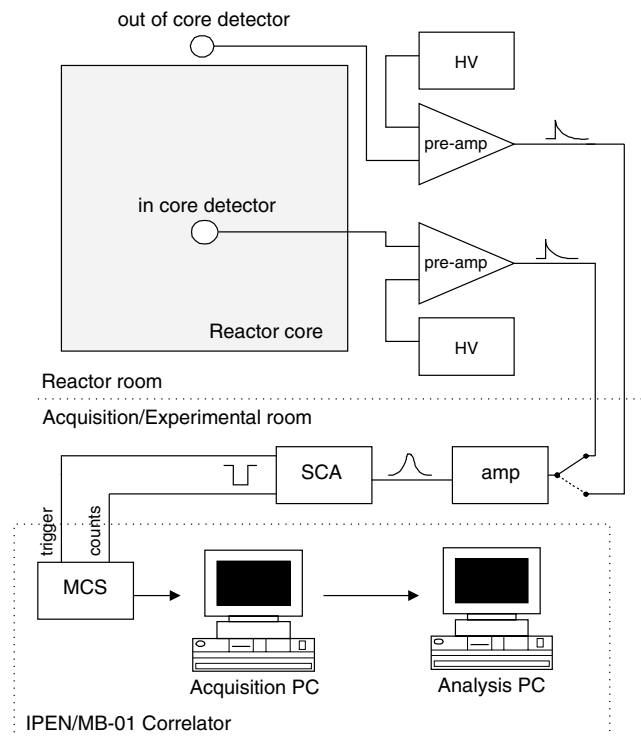


Fig. 4. Schematic diagram of the measurement system.

width and amplitude of 5 V into a 50 Ω load. A high-speed PCI-bus multi-channel counter card subsequently records the elapsed time between a trigger and subsequent pulses. The dwell time can be fixed as a minimum of 100 ns. The number of time bins (channels) is selectable from 4 to 65,536. Moreover, a dual-port memory on the MCS card

permits quick computer access to the spectral data for process purpose, without interrupting data acquisition. Software written in LabVIEW™ G-Language is used to control the acquisition. In order to sustain a satisfying acquisition rate, the features of the host PC is of high importance. For that reason, our acquisition PC is a 2.4 GHz processor PC which is dedicated only to the PCI bus of the timemarking card. Once the data has been collected, which corresponds to one MCS sweep, it is transferred to a second PC where the Feynman- α method was implemented on C/C++ language. In this way, our system provides an on-line data analysis because the writing and reading of the data from the MCS memory buffer are executed independently.

The Feynman- α distributions were obtained via the bunching technique proposed by Misawa et al. (1962) and revised by Kitamura et al. (2000). In this technique, neutrons counts within a fundamental counting gate time (dwell time) are accumulated in the MCS buffer, and neutron counts of longer gate widths are synthesized by bunching neutron counts in adjacent MCS channels. For example, when the dwell time was selected as T ms, the neutron count data stored in the adjacent channels of the MCS were bunched to obtain the count rate distribution of 2T ms intervals. The mean and variance values were calculated using the bunched data, then the Y-value in Eq. (16) was obtained. In this way, the Y-value can be calculated almost continuously as a function of the time interval. Furthermore, the Feynman- α distribution can be obtained immediately after each MCS sweep providing an on-line data analysis.

5. Measurements results

As mentioned in the previous section, the Feynman- α experiments were performed in two different core configurations, which are showed in Fig. 2. Firstly, according to Fig. 2a, measurements were conducted using a small BF3 detector vertically positioned in the center of the active region. In order to measure the ratio $\beta_{\text{eff}}/\Lambda$, Feynman- α distributions were recorded at three different subcritical levels near the delayed critical state. Each subcritical level was achieved by changing the control rods positions. In such measurements, the system was governed by its own intrinsic source. The intrinsic source strength is small enough to provide measurements of the Feynman- α distributions near criticality with a reasonable count rate in the detector which favors an accurate extrapolation to the critical condition. Fig. 5 shows the Feynman- α distribution recorded at -4.77 pcm. According to the two-region model predictions, near criticality the component driven by ω_7 root is dominant, and the Feynman- α distribution reduces to that derived through the one-region model. In this way, the prompt neutron decay constants α were obtained by fitting each Feynman- α distributions using a typical least-square algorithm to a function which includes only one exponential term. Fig. 6 shows the fitted α values vs. inverse

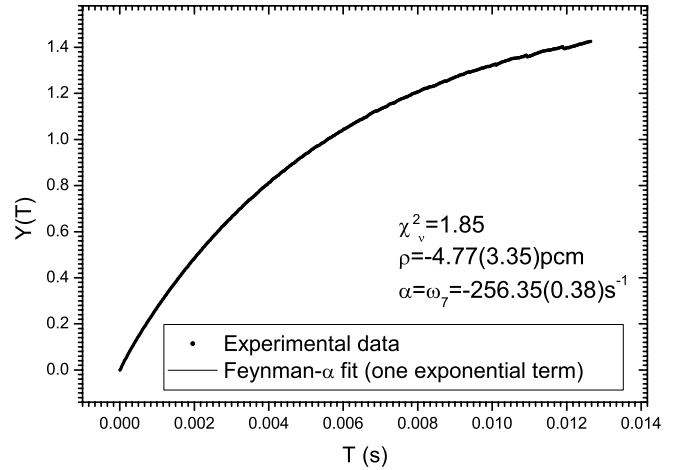


Fig. 5. Typical Feynman- α distribution for a subcritical level of -4.77 pcm.

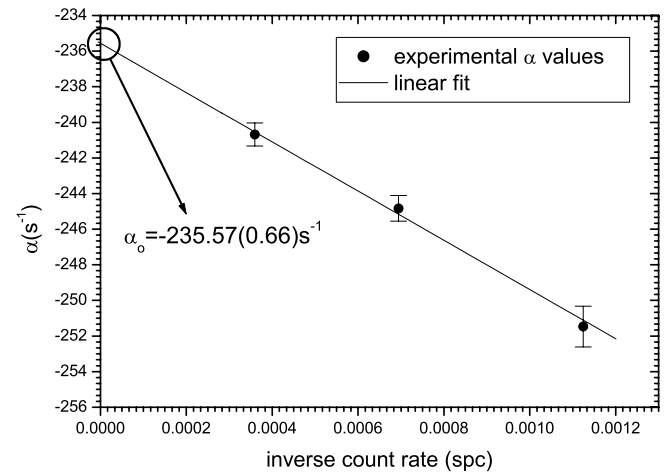


Fig. 6. Plot of the α values versus the inverse count rate.

count rate of the BF₃ detector used to perform the measurements. As mentioned before, by adopting the NSMM, the inverse count rate can be directly related to the subcritical reactivity through $\rho = \epsilon S/C$ for $\epsilon S/C \gg 1$. The relation between inverse count rates and measured α values was extrapolated to the critical condition and a $\beta_{\text{eff}}/\Lambda$ value was estimated as $-235.57(0.66) \text{ s}^{-1}$.

In the second core configuration illustrated in Fig. 2b, Feynman- α experiments were performed in a very large range of subcriticality, from -500 pcm to -25,000 pcm, approximately. This experimental setup was implemented in order to validate the two-region model predictions and obtain β_{eff} in an absolute experimental way. As presented in the previous section, deeply subcritical levels were reached loading eight burnable poison rods in the reactor core. In order to achieve the different reactivity levels, the system was perturbed with the insertion of all control and safety rods simultaneously in steps of 5%. Due to the significant variation in the neutron flux, two neutron detectors with different sensitivities were used to allow precise

measurements in reasonable length of times. More specifically, a boron-lined proportional counter was used at levels near the delayed critical condition and a more sensitive ^3He neutron detector at deeply subcritical levels. In addition, to increase the count rate of the detectors to a reasonable value, the startup source (Am–Be, 1Ci) was placed in the center of the core to drive the system during the measurements.

As predicted by the two-region model, the correlated component governed by the ω_7 root is dominant, and only one exponential term could be observed in the Feynman- α curves recorded in reflector region. Thus, the prompt neutron decay constant α was obtained by the least-square fitting of these curves to the theoretical formula, Eq. (16), with only the first exponential term. Fig. 7 shows the experimental results at -3363.76 pcm. At subcritical levels above -1000 pcm, approximately, detector dead time effects potentially distorted the initial channels of the Feynman- α curves. In Fig. 8, the Feynman- α distribution recorded at -499.88 pcm is shown. The effect of the dead time is clearly noticed at the beginning of the distribution where the Y -values are less than unit. Consequently, it was observed that the fitted α value was a function of the lower boundary of the fit interval. The beginning of the fit interval is therefore very crucial for the validity of the α values obtained from the least-square fit. Only the positive Y -values were considered in the fit procedure such that the dead time effects were completely removed. In Fig. 8, the arrow indicates the fit threshold position. In this case, the fit interval was taken from $T = 0.0003$ s up to $T = 0.0120$ s. In this way, the α value dependence on the lower limit of the fit interval was eliminated.

In Fig. 9, the fitted α values were plotted as a function of the inverse count rate ($1/C$). The $1/C$ values were obtained using a BF_3 neutron detector of 2.5 cm diameter \times 40 cm height and sensitivity of 23.1 cps/nv positioned in the same place where α values were measured and at the same control and safety rod position. As predicted by the two-region model, Fig. 9 shows that the prompt neutron decay constant did not follow a linear relationship with $1/C$. In fact, the behavior of the data presented in Fig. 9 can be described by Eq. (20). Again in accordance with the two-region model, the curve is bounded asymptotically by Eq. (10) in the vicinity of delayed critical and $1/\tau_r$ at deeply subcritical levels.

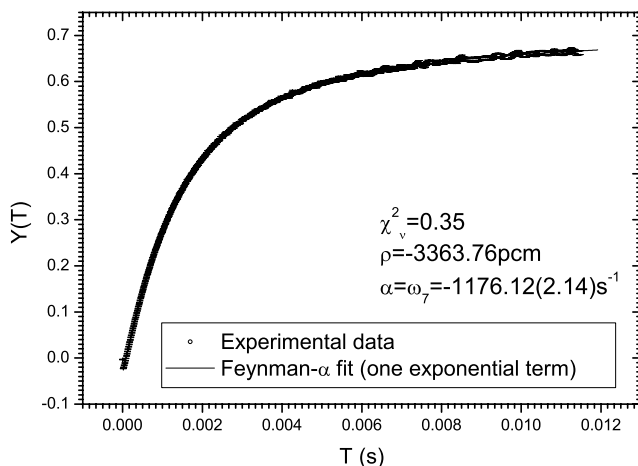


Fig. 7. Feynman- α distribution for a subcritical level of -3363.76 pcm.

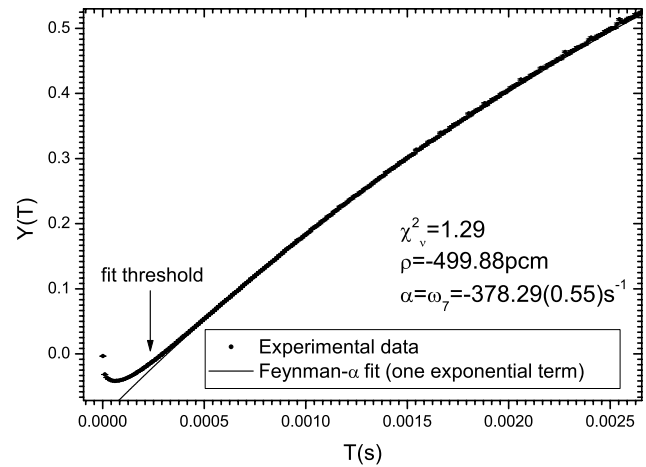


Fig. 8. Initial channels of the Feynman- α distribution for a subcritical level of -499.88 pcm.

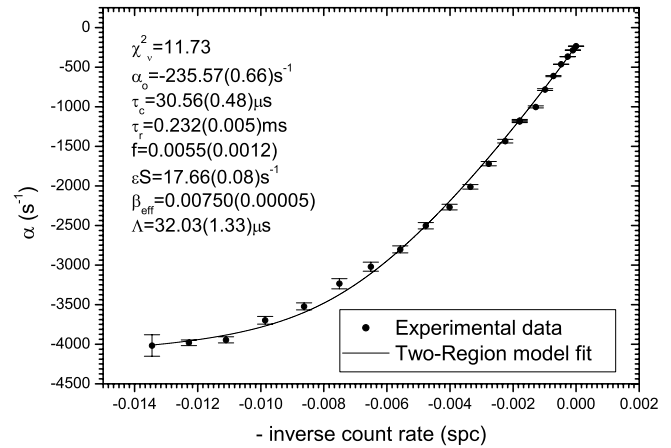


Fig. 9. The prompt neutron decay constant, α , vs. inverse count rate. The parameters were obtained via least-square fit using Eq. (20).

stant did not follow a linear relationship with $1/C$. In fact, the behavior of the data presented in Fig. 9 can be described by Eq. (20). Again in accordance with the two-region model, the curve is bounded asymptotically by Eq. (10) in the vicinity of delayed critical and $1/\tau_r$ at deeply subcritical levels.

The parameters α_0 , τ_c , τ_r , f and β_{eff} were directly obtained by fitting the data illustrated in Fig. 9 to Eq. (20) by the least-squares method. The solid line observed in Fig. 9 is the fit result, which agrees well with the experimental data. The quantity ϵS was also fitted by changing the reactivity ρ in Eq. (20) to $\epsilon S/C$. Table 1 summarizes the fitted parameters.

Through the knowledge of the fitted parameters τ_c , τ_r and f , the prompt neutron generation time can be obtained using Eqs. (5), (6) and (17), which results in $\Lambda = 32.02(0.58)$ μs . The reflector α_0 value was obtained substituting the fitted parameters τ_c , τ_r , f and β_{eff} in Eq. (20), and calculating for the critical state.

Table 1
Measured results

Parameter	Feynman- α (core measurements)	Feynman- α (reflector measurements)	Frequency analysis ^a	Frequency analysis ^b
α_0	$-235.57(0.66) \text{ s}^{-1}$	$-235.25(4.55) \text{ s}^{-1}$	$-234.61(3.26) \text{ s}^{-1}$	$231.00(0.94) \text{ s}^{-1}$
τ_c	–	$30.56(0.48) \mu\text{s}$	–	–
τ_r	–	$0.232(0.005) \text{ ms}$	–	–
f	–	$0.0055(0.0012)$	–	–
β_{eff}	–	$7.50(0.05) \times 10^{-3}$	$7.47(0.11) \times 10^{-3}$	$7.39(0.07) \times 10^{-3}$
Λ	–	$32.02(0.58) \mu\text{s}$	$32 \mu\text{s}$	$31.99(0.33) \mu\text{s}$

^a With delayed neutron (Diniz and dos Santos, 2006).

^b Without delayed neutron (dos Santos et al., 2006).

Table 1 also shows a comparison between the present results and those obtained by the frequency analysis technique (Diniz and dos Santos, 2006; dos Santos et al., 2006). The β_{eff} and Λ measured by the Feynman- α and the frequency analysis methods agreed well with each other when the standard deviations are considered. In the same way, the α_0 values measured in the present work agree with that measured by the frequency analysis with delayed neutron. For the frequency analysis method without delayed neutron, however, the α_0 is significantly smaller than that obtained from the Feynman- α measurements in core. The same discrepancy is also noticed in the β_{eff} given in the last column of Table 1. These discrepancies are probably due to a systematical error in the Diven factor which is used in the frequency analysis method without delayed neutron in order to derive the parameters.

The small standard deviations obtained in the present results show that precise absolute measurements for β_{eff} and Λ can be obtained. In fact, the uncertainty in β_{eff} is 0.67%, which is smaller than the proposed target accuracy of $\pm 3\%$ (1 s.d.) for this parameter.

In the IPEN/MB-01 research reactor nearly 97% of the total fissions are due to ^{235}U and out of that nearly 90% are thermal fissions. Thus, the thermal events in which ^{235}U is the only contributor, dominates the total number of fissions. In this way, it is expected that β_{eff} follow basically the ^{235}U thermal yield. This prediction is consistent with

results from TORT and MCNP-4C3 extracted from Diniz and dos Santos (2006) and summarized in Table 2.

Table 3 lists theory/experiment comparisons for the β_{eff} measured in this work. According to these results, JENDL3.3 presented the best performance and meets the desired accuracy for the calculation of this parameter. This result is in complete agreement with the adjustment study carried out by Sakurai and Okajima where the ^{235}U yield was reduced by 0.9% (Sakurai and Okajima, 2002).

6. Conclusions

On the basis of the Two-Region model and Feynman- α experiments, a new methodology for absolute measurement of the effective delayed neutron fraction β_{eff} was successfully developed in the IPEN/MB-01 research reactor. By adopting this approach, an absolute experimental determination of β_{eff} could be carried out with the required accuracy and without knowledge of any other parameter. In order to implement this technique, several Feynman- α distributions were recorded in core and reflector regions. According to the two-region model predictions, only one exponential component was observed in the Feynman- α distributions. Furthermore, it was noticed a nonlinear behavior between the prompt neutron decay constants α and the inverse count rate of the detector, which is also in agreement with the two-region model predictions. Hence, it was concluded that the kinetic behavior of the IPEN/MB-01 reactor core is well described by the two-region model. Based on the present approach, β_{eff} was evaluated with an uncertainty of 0.67%. This final result indicated that the new experimental technique can be successfully applied to measure β_{eff} values within the current target accuracy of $\pm 3\%$ (1 s.d.). In addition, the prompt neutron generation time Λ and other parameters, were also measured in a purely experimental way. The parameters β_{eff} and Λ are in good agreement with the values found from other experiments. However, the β_{eff} value given by frequency analysis method neglecting delayed neutrons is lower than that measured in the present work. Probably, systematical uncertainties in the Diven factor, which is used in the β_{eff} derivation from the frequency analysis experiments, could result in such discrepancy. The C/E values for the β_{eff} measured in this work show that JENDL3.3 presented the best agreement. More precisely, it was

Table 2
Final calculated results for β_{eff} given by TORT (S₁₆ and 16 groups) (Diniz and dos Santos, 2006)

		ENDF/B-VI.8 ^a	JEFF-3.1	JENDL 3.3
β_{eff} (pcm)	TORT	792.38	774.38	756.16
	MCNP-4C3	781.6 ± 4.1	771.7 ± 4.1	755.6 ± 4.0
^{235}U Thermal yield		1.670×10^{-2}	1.620×10^{-2}	1.585×10^{-2}

^a LANL review.

Table 3
Comparison of the calculated β_{eff} with the experimental value

		ENDF/B-VI.8 ^a	JEFF-3.1	JENDL 3.3
β_{eff} (C/E)	TORT	1.0565	1.0325	1.0082
	MCNP-4C3	1.0421	1.0289	1.0074

^a LANL review.

noticed that the agreement with calculated β_{eff} values made using JENDL3.3 is within 1%. This result justifies the adjustment study performed by Okajima and Sakurai where the ^{235}U yield was reduced by 0.9%.

Acknowledgements

The authors are grateful for financial support from the Fundação de Amparo à Pesquisa do Estado de São Paulo (FAPESP) under Contracts 03/01261-0 and 04/14542-0.

The authors thank the operational staff of the IPEN/MB-01 reactor for their patience and efficient operation during the course of the experiment.

References

- Avery, R., 1958. Theory of coupled reactors. In: Proceedings of the 2nd International Conference on Peaceful Uses Atomic Energy, vol. 12, Geneva, Switzerland, p. 182.
- Avery, R. et al., 1958. Coupled fast-thermal power breeder critical experiment. Nucl. Sci. Eng. 3 (2), 129–144.
- Bell, G.I., Glasstone, S., 1970. Nuclear Reactor Theory. Van Nostrand Reinhold Company, New York.
- Brunson, G.S., 1975. On the possible connection between the central worth discrepancy and the dollar discrepancy. Nucl. Instrum. Methods 125, 139–147.
- Brunson, G.S., Huber, R.J., 1975. Two-region analysis of pulsing data in fast critical systems. Nucl. Instrum. Methods 128, 379–403.
- Busch, D., Spriggs, G.D., 1994. Preliminary results of a Rossi-alpha experiment on the University of New Mexico's AGN-201 Experiment. Trans. Am. Nucl. Soc. 71, 459–460.
- Butterfield, K.B., 1994. The SHEBA experiment. Trans. Am. Nucl. Soc. 74, 199–200.
- Coats, R.L., 1967. Neutronic decoupling of fast-burst reactors. Trans. Am. Nucl. Soc. 10 (1), 243.
- Cohn, C.E., 1961. Reflected-reactor kinetics. Trans. Am. Nucl. Soc. 4 (1), 73.
- Cohn, C.E., 1962. Reflected-reactor kinetics. Nucl. Sci. Eng. 13, 12–17.
- D'Angelo, A., 2002. Overview of the delayed neutron data activities and results monitored by the NEA/WPEC subgroup 6. Prog. Nucl. Energy 41 (1–4), 5–38.
- D'Angelo, A., Rowlands, J.L., 2002. Conclusions concerning the delayed neutron data for the major actinides. Prog. Nucl. Energy 41 (1–4), 391–412.
- Diniz, R., 2005. Obtenção das constantes de decaimento e abundâncias relativas de nêutrons atrasados através da análise de ruído em reatores de potência zero. Tese de doutorado – IPEN, São Paulo, Brazil.
- Diniz, R., dos Santos, A., 2006. Experimental determination of the decay constants and abundances of delayed neutrons by means of reactor noise analysis. Nucl. Sci. Eng. 152 (2), 125–141.
- dos Santos, A. et al., 1999. The inversion point of the isothermal reactivity coefficient of the IPEN/MB-01 Reactor-I: experimental procedure. Nucl. Sci. Eng. 133, 314–326.
- dos Santos, A. et al., 2006. A proposal of a benchmark for β_{eff} , β_{eff}/A and A of thermal reactors fueled with slight enriched uranium. Ann. Nucl. Energy 33, 848–855.
- dos Santos, A., et al., 2004. LEU-COMP-THERM-077 critical loading configurations of the IPEN/MB-01 Reactor. In: Blair Briggs, J. (Ed.), International Handbook of Evaluated Criticality Safety Benchmark Experiments, September Ed. Nuclear Energy Agency, Paris, NEA/NSC/DOC (95)03/1.
- Feynman, R.P. et al., 1956. Dispersion of the neutron emission in U-235 Fission. J. Nucl. Energy 3, 64–69.
- Fort, E. et al., 2002. Recommended values of the delayed neutron yield for: U-235; U-238 and Pu-239. Prog. Nucl. Energy 41 (1–4), 317–359.
- Gamble, D.P., 1960. The effect of reflector-moderated neutrons on the kinetics of the kinetic experiment water boiler reactor. Trans. Am. Nucl. Soc. 3 (1), 122.
- Jammes, C. et al., 2002. First MUSE-4 experimental results based on time series analysis. PHYSOR 2002, Seoul, Korea, (October), pp. 7–10.
- Kaneko, Y. et al., 1988. Evaluation of delayed neutron data for thermal fission of U-235 based on integral experiments at semi-homogeneous experiment. J. Nucl. Sci. Technol. 25, 673–681.
- Karam, R.A., 1964. Measurement of Rossi-alpha in reflected reactors. Trans. Am. Nucl. Soc. 7 (2), 283.
- Karam, R.A., 1965. Spatial dependence of the decay rates of prompt-neutron chains in reflected reactors. Trans. Am. Nucl. Soc. 8 (1), 224.
- Kitamura, Y. et al., 2000. General formulae for the Feynman- α method with the bunching technique. Ann. Nucl. Energy 27, 1199–1216.
- Litaize, O., Santamarina, A., 2001. Experimental validation of the effective delayed neutron fraction in the MISTRAL1-UOX and MISTRAL2-MOX Homogeneous Core. JEFDOC-872.
- Long, R.L., 1965. Effects of reflectors on the burst characteristics of the white sands missile range (WSMR) fast-burst reactor. Trans. Am. Nucl. Soc. 8 (2), 451.
- Misawa, T., Unesaki, H., 2003. Measurement of subcriticality by higher mode source multiplication method. In: Proceedings of the International Conference on Nuclear Critical Safety (ICNC2003).
- Misawa, T. et al., 1962. Measurement of prompt neutron decay constant and large subcriticality by the Feynman- α method. Nucl. Sci. Eng. 104, 53–65.
- Nakajima, K., 2001. Re-evaluation of the effective delayed neutron fraction measured by the substitution technique for a light water moderated low-enriched uranium core. J. Nucl. Sci. Technol. 38, 1120–1125.
- Price, C.C., 1970. Prompt neutron decay constants in a reflected fast burst reactor. Dissertation, University of New Mexico.
- Rudstan, G. et al., 2002. Delayed neutron data for major actinides. NEA/WPEC-6 Report. pp. 1–130.
- Sakurai, T. et al., 1999. Experimental cores for benchmark experiments of effective delayed neutron fraction β_{eff} at FCA. Prog. Nucl. Energy 35 (2), 131–156.
- Sakurai, T., Okajima, S., 2002. Adjustment of total delayed neutron yields of ^{235}U , ^{238}U and ^{239}Pu in JENDL-3.2 using benchmark experiments on effective delayed neutron fraction, β_{eff} . J. Nucl. Sci. Technol. 39 (1), 19–30.
- Shi, Yong-Qian et al., 2005. Review and research of the neutron source multiplication method in nuclear critical safety. Nucl. Technol. 149 (1), 122–127.
- Spriggs, G.D., 1977. A measurement of the effective delayed neutron fraction of the Westinghouse Idaho nuclear company slab tank assembly using Rossi- α techniques. Nucl. Sci. Eng. 62, 105–106.
- Spriggs, G.D. et al., 1997. Two-region kinetic model for reflected reactors. Ann. Nucl. Energy 24 (3), 205–250.
- Takano, M. et al., 1985. Analysis of SHE critical experiments by neutronic design codes for experimental very high temperature reactor. J. Nucl. Sci. Technol. 22, 358–370.
- Tonoike, K. et al., 2002. Kinetic parameters β_{eff}/A measurement on low enriched uranyl nitrate solution with single unit cores (600 ϕ , 280T, 800 ϕ) of STACY. J. Nucl. Sci. Technol. 39, 1227–1236.
- Uhrig, R.E., 1970. Random Noise Techniques in Nuclear Reactor System. The Ronald Press Company.
- Van der Marck, S., 2006. β_{eff} calculations using ENDF/B-VII beta2 nuclear data. NRG 21616/05.70024/P, Petten, June 13.
- Van der Marck, S. et al., 2004. Benchmark results for delayed neutron data. In: Proceedings of International Conference on Nuclear Data for Science and Technology, Santa Fe, USA.
- Williams, T. et al., 1996. Experimental investigation of the kinetic parameter β_{eff}/A in graphite-moderated, LEU fueled, critical configurations. In: Proceedings of the International Conference on the Physics of Reactors (PHYSOR 96), September 16–20, Mito, Ibaraki, Japan, 2, E200.
- Yamane, Y., 1996. Feynman- α formula with dead time effect for a symmetric coupled-core system. Ann. Nucl. Energy 23 (12), 981–987.